

Shear Waves in an Initially Stressed Elastic Plate with Periodic Corrugations

Muhammad A. Hawwa¹ 

Received: 26 July 2016 / Accepted: 13 October 2016 / Published online: 27 October 2016
© King Fahd University of Petroleum & Minerals 2016

Abstract The influence of the combined effect of initial stress and periodic surface corrugation on ultrasonic SH wave propagation in an elastic plate is investigated. Considering weak surface corrugations, a small parameter is defined using the ratio between the corrugation amplitude and the average thickness of the plate and the perturbation method of strained parameters is used up to the second order. An equation for evaluating the wave phase velocity in the periodically corrugated plate is realized. Numerical examples are provided to graphically illustrate the variations of the phase velocity in periodic plates, with various corrugation amplitudes and wavelengths, under compressive and tensile initial stresses over a frequency spectrum. The study reveals the dispersive nature of SH waves in corrugated plates. It is found that the wave phase velocities are slightly higher (lower) in plates under initial tension (compression) than initially stress-free plates. The influence of initial stresses on SH phase speed decreases as the frequency increases. It is shown that periodic surface roughness has a stronger effect on reducing wave phase speeds than a shallow surface waviness.

Keywords SH waves · Weakly corrugated plates · Dispersion · Initial stress · Perturbation methods

1 Introduction

The effect of initial stresses on elastic wave propagation characteristics has been an active research topic over the past decades. Initial stresses normally occur in plates during their manufacturing and/or assembly. A dominant method for nondestructively evaluating plates is the use of elastic (ultrasonic) wave propagation characteristics, which provide valuable information about the internal composition of their structures, their interfaces as well as the conditions of their boundary surfaces. Accounting for the influence of initial stress on material characterization and nondestructive testing is important in light of the fact that theoretical studies so far showed a clear influence of initial stresses on elastic wave dispersion and stability, especially at low frequency.

An early theoretical study by Wagh [1] was based on Cauchy's model to study the effect of initial compression across an elastic layer thickness on the zeroth-order SH mode. Zhuk [2] studied the influence of finite initial strain on the phase speeds of SH and torsional waves in an elastic layer having an arbitrary form of elastic potential. Wilson [3] presented the derivation of approximate dispersion equations valid when the wavelength was much greater than the plate thickness and stability implications. Later, Ogden and Roxburgh [4,5] focused on the aspects of dynamic stability in a pre-stressed plate with a general form of strain energy function. Rogerson and Fu [6] obtained asymptotic expansions for the wave speed as a function of wavenumber and initial stress in plates satisfying neo-Hookean and Mooney–Rivlin strain energy functions. Sandiford and Rogerson [7] derived asymptotic expressions of the dispersion relation and elucidation of the longitudinal wave front in slightly compressible pre-strained elastic plate. Pichugin [8] wrote a dissertation on asymptotic wave models in initially stressed elastic layers with fixed and free faces. Kaplunov et al. [9–11] used

✉ Muhammad A. Hawwa
drmafah@kfupm.edu.sa

¹ Department of Mechanical Engineering, King Fahd University of Petroleum and Minerals, Dhahran 31261, Saudi Arabia

asymptotic models up to the third order to study the influence of initial stress on wave propagation in isotropic elastic layers with free as well as fixed faces. Nolde et al. [12] utilized asymptotic analysis to note that the existence of initial stress in a plate could allow the speed of the longitudinal wave front to be equal to or less than its correspondent shear wave. Wijeyewickrema et al. [13] considered an initially stressed constrained layer and studied the influence of constraining degree on dispersive behavior. Zhang and Yu [14] presented dispersion curves in a plate having two types of initial stresses including a homogeneous stress in the thickness direction and inhomogeneous stress in the wave-propagating direction. Pau and di Scalea [15] analyzed Lamb wave propagation in an elastic plate with initial stresses in the direction of the wave propagation and in an orthogonal to the wave propagation direction. They presented the variation of phase and group velocity as a function of the initial stress.

Other researchers focused on wave propagation in fiber-reinforced and layered plates. Rogerson and Sandiford [16] analyzed extensional waves in a four-ply laminated plate and showed that the asymptotic limits of the fundamental wave velocity were either a surface or interfacial wave speed. Akbarov et al. [17] used harmonic potentials to study Lamb waves in an initially strained sandwich plate and estimated the influence of the magnitude of the initial strains on the wave propagation velocity. Wijeyewickrema and Leungvicharoen [18] considered an initially stressed three-layered composite plate with imperfectly bonded interfaces and studied the effect of weak bonding on dispersive behavior. Kayestha and Wijeyewickrema [19] studied the coupled symmetric–antisymmetric dispersion in an initially stressed bilayered plate. Kayestha et al. [20] compared elastic wave propagation along a nonprincipal direction to waves propagating along a principal direction in an initially stressed, traction free layer. Zamanov and Agasiyev [21] examined the dispersive behavior of Lamb waves in an initially strained three-layer plate and obtained numerical results for a harmonic potential. Akbarov et al. [22] considered an initially strained elastic sandwich plate under two cases of loading, a dead load that contributed an initial stress and a follower load that contributed the initial stress while constraining Lamb wave propagation in the plate. Son and Kang [23] analyzed shear wave propagation in an initially stressed elastic layer that was bonded to a piezoelectric layer. Yu and Li [24] analyzed Lamb-like waves and SH waves in initially stressed multilayered plates showing that the influence of initial stress in the thickness direction was significantly different from that in the longitudinal direction.

In all of the above-covered research, initially stressed elastic plates were considered to have straight surfaces and interfaces. The present paper aims at studying wave propagation in an initially stressed plate with uneven surfaces. Since it is common to encounter plate-machining defects that lead

to the formation of small surface corrugations, the combined effect of initial stresses and surface corrugations on elastic wave propagation needs a rigorous analysis. As an initial phase of investigation, this study focuses on the influence of initial stresses in a periodically corrugated plate on the phase speed of horizontally polarized shear (SH) waves. Assuming that the surface corrugations have a small amplitude allows utilizing asymptotic expansions in terms of a small geometric parameter. An analytical formula is derived for the elastic SH wave phase velocity. The effect of initial tensile and compressive stresses on the wave phase speed in plates having sinusoidal surface corrugations with different amplitudes and wavelengths is presented.

2 Mathematical Model and Solution

Let us consider an elastic plate with sinusoidally corrugated surfaces under an initial stress in the Cartesian frame of reference $(\hat{x}, \hat{y}, \hat{z})$ as shown in Fig. 1. The lower and upper plate surfaces are described by $\hat{z} = \hat{a} \sin(\hat{k}_s \hat{x})$ and $\hat{z} = \hat{h} + \delta \hat{a} \sin(\hat{k}_s \hat{x} + \theta)$, respectively, where \hat{h} is the average thickness of the plate, \hat{k}_s is the wavenumber of the periodic surface corrugation of the plate, \hat{a} is the amplitude of corrugation, and to allow analysis generality θ is a phase angle between the two plate periodic surfaces and δ is a coefficient allowing a different corrugation amplitude at each plate surface. The horizontally polarized motion of the plate is described by the following governing equation of motion [25]:

$$C_{66} \frac{\partial^2 \hat{v}}{\partial \hat{x}^2} + C_{44} \frac{\partial^2 \hat{v}}{\partial \hat{z}^2} \mp \frac{P}{2} \frac{\partial^2 \hat{v}}{\partial \hat{x}^2} = \rho \frac{\partial^2 \hat{v}}{\partial t^2} \quad (1)$$

where t is the time coordinate, \hat{v} is the displacement in the \hat{y} -direction, ρ is the material density, C_{44} and C_{66} are the elastic shear moduli of the anisotropic (orthotropic) material of the plate, P is the initial stress on the plate in the \hat{x} -direction, and positive and negative signs indicate tensile and compressive initial stresses, respectively. The governing equation of motion is supplemented by the boundary conditions of the vanishing of the stress vector component normal to the corrugated plate surfaces

$$C_{66} \frac{\partial \hat{v}}{\partial \hat{x}} n_x + C_{44} \frac{\partial \hat{v}}{\partial \hat{z}} n_z = 0 \quad \text{at lower surface,} \\ \hat{z} = \hat{a} \sin(\hat{k}_s \hat{x}) \quad (2a)$$

$$C_{66} \frac{\partial \hat{v}}{\partial \hat{x}} n_x + C_{44} \frac{\partial \hat{v}}{\partial \hat{z}} n_z = 0 \quad \text{at upper surface,} \\ \hat{z} = \hat{h} + \delta \hat{a} \sin(\hat{k}_s \hat{x} + \theta) \quad (2b)$$

where (n_x, n_z) are the components of unit outward-pointing vector normal to the corrugated surfaces.

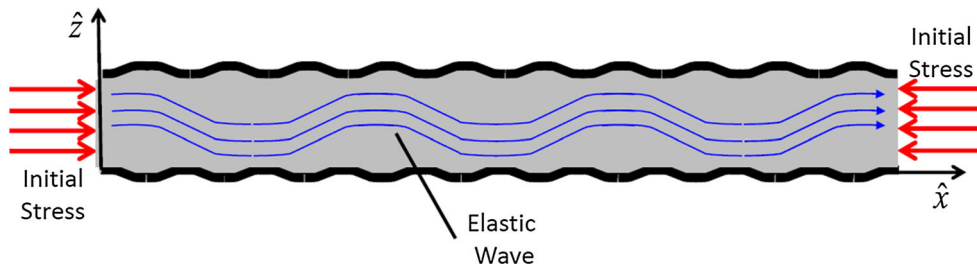


Fig. 1 The weakly corrugated plate. The initial stress could be tensile or compressive

Focusing on the propagation of a horizontally polarized time-harmonic ultrasonic wave along the plate in the \hat{x} -direction, then the displacement is described by $\hat{v} = \hat{V}e^{-i\omega t}$ where \hat{V} is the displacement amplitude and ω is the angular frequency. If one takes the average plate thickness \hat{h} to be a spatial reference quantity, the equation of motion for a shear wave in the plate and the boundary conditions can then be written in the following dimensionless form:

$$\frac{\partial^2 V}{\partial z^2} + \left(\frac{C_{66}}{C_{44}} \mp \frac{P}{2C_{44}} \right) \frac{\partial^2 V}{\partial x^2} = -\frac{\rho\omega^2\hat{h}^2}{C_{44}} V \tag{3a}$$

$$\frac{\partial V}{\partial z} = \frac{C_{66}}{C_{44}} \varepsilon k_s \cos(k_s x) \frac{\partial V}{\partial x} \quad \text{at} \quad z = \varepsilon \sin(k_s x) \tag{3b}$$

$$\frac{\partial V}{\partial z} = \frac{C_{66}}{C_{44}} \varepsilon \delta k_s \cos(k_s x + \theta) \frac{\partial V}{\partial x} \quad \text{at} \quad z = 1 + \varepsilon \delta \sin(k_s x + \theta) \tag{3c}$$

where all quantities without carets in (3) are dimensionless quantities, and $\varepsilon (= \hat{a}/\hat{h})$ is the ratio of the amplitude of the surface corrugation to the average thickness of the plate. ε is considered to be a small dimensionless parameter since the surface corrugations are considered to be weak.

In order to simplify boundary conditions (3b and 3c), they can be expanded using Taylor series around $z = 0$ and $z = 1$, respectively. This leads to transferring the boundary conditions to the average line of the sinusoidally corrugated upper and lower surfaces of the plate. Hence, the system of equations (3) takes the following form:

$$\frac{\partial^2 V}{\partial z^2} + R \frac{\partial^2 V}{\partial x^2} + \kappa^2 V = 0 \tag{4a}$$

$$\begin{aligned} \frac{\partial V}{\partial z}(x, 0) = & -\varepsilon \sin(k_s x) \frac{\partial^2 V}{\partial z^2}(x, 0) \\ & - \frac{1}{2} \varepsilon^2 \sin^2(k_s x) \frac{\partial^3 V}{\partial z^3}(x, 0) + \frac{C_{66}}{C_{44}} \varepsilon k_s \cos(k_s x) \left[\frac{\partial V}{\partial x}(x, 0) \right. \\ & \left. + \varepsilon \sin(k_s x) \frac{\partial^2 V}{\partial x \partial z}(x, 0) + \frac{1}{2} \varepsilon^2 \sin^2(k_s x) \frac{\partial^3 V}{\partial x \partial z^2}(x, 0) \right] \end{aligned} \tag{4b}$$

$$\begin{aligned} \frac{\partial V}{\partial z}(x, 1) = & -\varepsilon \delta \sin(k_s x + \theta) \frac{\partial^2 V}{\partial z^2}(x, 1) \\ & - \frac{1}{2} \varepsilon^2 \delta^2 \sin^2(k_s x + \theta) \frac{\partial^3 V}{\partial z^3}(x, 1) \\ & + \frac{C_{66}}{C_{44}} \varepsilon \delta k_s \cos(k_s x + \theta) \left[\frac{\partial V}{\partial x}(x, 1) \right. \\ & \left. + \varepsilon \delta \sin(k_s x + \theta) \frac{\partial^2 V}{\partial x \partial z}(1, 0) \right. \\ & \left. + \frac{1}{2} \varepsilon^2 \delta^2 \sin^2(k_s x + \theta) \frac{\partial^3 V}{\partial x \partial z^2}(x, 1) \right] \end{aligned} \tag{4c}$$

where $\kappa (= \omega\hat{h}/c_0)$ is the nondimensional wavenumber, $c_0 = \sqrt{\frac{C_{44}}{\rho}}$ is the bulk shear velocity of the plate material, and $R = (C_{66} \mp \frac{P}{2})/C_{44}$.

2.1 Asymptotic Formulation

The system of Eqs. (4a–4c) comprises a partial differential equation with nonhomogeneous boundary conditions. Perturbation methods are commonly utilized to obtain solutions for inhomogeneous systems of differential equations [26]. Therefore, the implementation of an asymptotic scheme for obtaining an approximate analytical solution can be done using the small parameter ε as a perturbation parameter to come up with an asymptotic solution for system (4). The analysis is done in two steps. The first is to use a straightforward perturbation scheme, which helps in identifying the uniformity of the asymptotic expansion, and the second is to expand the wavenumber as a strained parameter to obtain an asymptotic estimation for it.

2.1.1 Straightforward Asymptotic Expansion

The displacement V can be expanded in terms of ε as $V = V_0 + \varepsilon V_1 + \varepsilon^2 V_2 + \dots$. Upon the substitution of this expansion into Eqs. (4a–4c), it is found that the asymptotic expansion breaks down at the first level of approximation when the wavenumber of the propagating SH mode equals half of the periodic surface corrugation wavenumber k_s . This condition is known in the literature as Bragg resonance [27], which occurs as a result to the formation of a stopband in

the dispersion spectrum of the periodic waveguide (the plate with periodic surface corrugations). In a banded dispersion spectrum, waves can propagate if their frequency is within a passband, and they cease to propagate if their frequency is within the stopband. The SH waves stopband behavior was considered by Hawwa and Asfar [28] for the case of single surface periodicity and by Hawwa [29] for the case of two surface periodicities. In this paper, it is intended to study the behavior of SH waves that are capable of propagation within frequency passbands. Therefore, one does not only need to seek a solution for V , but also one needs to seek a solution for the wavenumber κ .

2.1.2 Asymptotic Method of Strained Parameters

In order to seek uniform asymptotic expansions for the displacement and the wavenumber terms of ε , let us assume

$$V = V_0 + \varepsilon V_1 + \varepsilon^2 V_2 + \dots \quad (5)$$

$$\kappa = \kappa_0 + \varepsilon \kappa_1 + \varepsilon^2 \kappa_2 + \dots \quad (6)$$

The motivation of expanding the nondimensional wavenumber stems from the fact that surface corrugations are expected to influence wave phase velocity in the corrugated plate. By substituting Eqs. (5) and (6) into system (4) and equating coefficients of equal powers of ε on both sides of the equations, one can determine more accurate approximations in a successive fashion in a typical manner of the perturbation method of strained parameters. Thus, one has to solve the following three systems of equations sequentially:

Zeroth-Order Problem

$$\frac{\partial^2 V_0}{\partial z^2} + R \frac{\partial^2 V_0}{\partial x^2} + \kappa_0^2 V_0 = 0 \quad (7a)$$

$$\frac{\partial V_0}{\partial z}(x, 0) = 0 \quad (7b)$$

$$\frac{\partial V_0}{\partial z}(x, 1) = 0 \quad (7c)$$

First-Order Problem

$$\frac{\partial^2 V_1}{\partial z^2} + R \frac{\partial^2 V_1}{\partial x^2} + \kappa_0^2 V_1 = -(2\kappa_0 \kappa_1) V_0 \quad (8a)$$

$$\begin{aligned} \frac{\partial V_1}{\partial z}(x, 0) = & -\sin(k_s x) \frac{\partial^2 V_0}{\partial z^2}(x, 0) \\ & + \frac{C_{66}}{C_{44}} k_s \cos(k_s x) \frac{\partial V_0}{\partial x}(x, 0) \end{aligned} \quad (8b)$$

$$\begin{aligned} \frac{\partial V_1}{\partial z}(x, 1) = & -\delta \sin(k_s x + \theta) \frac{\partial^2 V_0}{\partial z^2}(x, 1) \\ & + \frac{C_{66}}{C_{44}} \delta k_s \cos(k_s x + \theta) \frac{\partial V_0}{\partial x}(x, 1) \end{aligned} \quad (8c)$$

Second-Order Problem

$$\begin{aligned} \frac{\partial^2 V_2}{\partial z^2} + R \frac{\partial^2 V_2}{\partial x^2} + \kappa_0^2 V_2 = & -(2\kappa_0 \kappa_1) V_1 \\ & - (\kappa_1^2 + 2\kappa_0 \kappa_2) V_0 \end{aligned} \quad (9a)$$

$$\begin{aligned} \frac{\partial V_2}{\partial z}(x, 0) = & -\sin(k_s x) \frac{\partial^2 V_1}{\partial z^2}(x, 0) \\ & - \frac{1}{2} \sin^2(k_s x) \frac{\partial^3 V_0}{\partial z^3}(x, 0) + \frac{C_{66}}{C_{44}} k_s \cos(k_s x) \\ & \times \left[\frac{\partial V_1}{\partial x}(x, 0) + \sin(k_s x) \frac{\partial^2 V_0}{\partial x \partial z}(x, 0) \right] \end{aligned} \quad (9b)$$

$$\begin{aligned} \frac{\partial V_2}{\partial z}(x, 1) = & -\delta \sin(k_s x + \theta) \frac{\partial^2 V_1}{\partial z^2}(x, 1) \\ & - \frac{1}{2} \delta^2 \sin^2(k_s x + \theta) \frac{\partial^3 V_0}{\partial z^3}(x, 1) \\ & + \frac{C_{66}}{C_{44}} \delta k_s \cos(k_s x + \theta) \left[\frac{\partial V_1}{\partial x}(x, 1) \right. \\ & \left. + \delta \sin(k_s x + \theta) \frac{\partial^2 V_0}{\partial x \partial z}(1, 0) \right] \end{aligned} \quad (9c)$$

In the sequel, the above three systems of equations are solved in a sequence.

2.2 Zeroth-Order Solution

Equations (7a–7c) admit a solution of the form

$$V_0 = A_n \cos(n\pi z) e^{ik_n x} \quad (10)$$

where A_n and k_n are the amplitude and the wavenumber of the n th propagation ultrasonic SH mode. The substitution of the assumed solution (10) into the boundary conditions (7b and 7c) leads to the following dispersion relation:

$$\frac{\omega \hat{h}}{c_0} - R k_n^2 = (n\pi)^2 \quad (11)$$

2.3 First-Order Solution

In order to deal with the first-order system (8), let us assume a particular solution for V_1 can be postulated in the form

$$V_1(x, z) = \Phi_1(z) e^{ik_n x} + \Phi_2(z) e^{i(k_n + k_s)x} + \Phi_3(z) e^{i(k_n - k_s)x} \quad (12)$$

Substituting the zeroth-order solution and (10) and assumed first-order solution (12) into the system of equations (8) and equating the coefficients of $e^{ik_n x}$, $e^{i(k_n + k_s)x}$, and $e^{i(k_n - k_s)x}$ yield three problems in Φ_1 , Φ_2 , and Φ_3 , as follows:

$$\Phi_1''(z) + (n\pi)^2\Phi_1(z) = -(2\kappa_0\kappa_1)A_j \cos(n\pi z) \tag{13a}$$

$$\frac{\partial\Phi_1}{\partial z}(0) = 0 \tag{13b}$$

$$\frac{\partial\Phi_1}{\partial z}(1) = 0 \tag{13c}$$

$$\Phi_2''(z) + [k_0^2 - R(k_n + k_s)^2]\Phi_2(z) = 0 \tag{14a}$$

$$\Phi_2'(0) = \left[-\frac{(n\pi)^2}{2} + i\frac{k_n k_s}{2} \frac{C_{66}}{C_{44}}\right] A_n \tag{14b}$$

$$\Phi_2'(1) = \delta(-1)^n \left[-\frac{(n\pi)^2}{2} + i\frac{C_{66}}{C_{44}} \frac{k_s k_n}{2} e^{i\theta}\right] A_n \tag{14c}$$

$$\Phi_3''(z) + [k_0^2 - R(k_n - k_s)^2]\Phi_3(z) = 0 \tag{15a}$$

$$\Phi_3'(0) = \left[-\frac{(n\pi)^2}{2} + i\frac{k_n k_s}{2} \frac{C_{66}}{C_{44}}\right] A_n \tag{15b}$$

$$\Phi_3'(1) = (-1)^n \delta \left[-\frac{(n\pi)^2}{2} + i\frac{k_n k_s}{2} \frac{C_{66}}{C_{44}}\right] e^{-i\theta} A_n \tag{15c}$$

Equation (13a–13c) comprises an ordinary inhomogeneous differential equation with homogeneous boundary conditions. One can multiply the governing equation (13a) by $\cos(n\pi z)$ and integrate by parts from $z = 0$ to $z = 1$ and invoke the boundary conditions (13b, 13c). This leads to determining the first-order approximation of the wavenumber. It is found that $k_1 = 0$, which indicates that the periodic surface corrugations do not influence the wavenumber at first-order level of approximation. Hence, a higher-order correction is needed to describe the effect of surface corrugations on the phase speed.

It remains to solve systems (14) and (15). The governing equations (14a) and (15a), respectively, admit solutions of the forms

$$\Phi_2(z) = b_{21}e^{ip_2z} + b_{22}e^{-ip_2z} \quad \text{where} \tag{16}$$

$$p_2 = \sqrt{k_0^2 - R(k_n + k_s)^2}$$

and

$$\Phi_3(z) = b_{31}e^{ip_3z} + b_{32}e^{-ip_3z} \quad \text{where} \tag{17}$$

$$p_3 = \sqrt{k_0^2 - R(k_n - k_s)^2}$$

In order to determine the unknown coefficients in the above-assumed solutions, one substitutes the solution (16) into the boundary conditions (14b, 14c), and the solution (17) into the boundary conditions (15b, 15c) to obtain the following solutions for coefficients:

$$\begin{pmatrix} b_{21} \\ b_{22} \end{pmatrix} = \frac{1}{2i \sin p_2} \begin{pmatrix} -e^{-ip_2} & 1 \\ -e^{ip_2} & 1 \end{pmatrix} \times \begin{pmatrix} \left[i\frac{(n\pi)^2}{2p_2} + \frac{k_n k_s}{2p_2} \frac{C_{66}}{C_{44}} \right] \\ (-1)^n \left[i\frac{(n\pi)^2}{2p_2} + \frac{k_s k_n}{2p_2} \frac{C_{66}}{C_{44}} \right] \delta e^{i\theta} \end{pmatrix} A_n \tag{18}$$

$$\begin{pmatrix} b_{31} \\ b_{32} \end{pmatrix} = \frac{1}{2i \sin p_3} \begin{pmatrix} -e^{-ip_3} & 1 \\ -e^{ip_3} & 1 \end{pmatrix} \times \begin{pmatrix} \left[i\frac{(n\pi)^2}{2p_3} + \frac{k_n k_s}{2p_3} \frac{C_{66}}{C_{44}} \right] \\ (-1)^n \left[i\frac{(n\pi)^2}{2p_3} + \frac{k_n k_s}{2p_3} \frac{C_{66}}{C_{44}} \right] \delta e^{-i\theta} \end{pmatrix} A_n \tag{19}$$

2.4 Second-Order Solution

At the second level of approximation, one has to find a solution for system (9). Let us seek a solution for V_2 in the form $V_2(x, z) = \Psi_2(z)e^{ik_n x}$, which upon substitution in the system of equations (9a–9c) leads to

$$\Psi_2''(z)e^{ik_n x} + [\kappa_0^2 - k_n^2 R]\Psi_2(z)e^{ik_n x} = -(\kappa_1^2 + 2\kappa_0\kappa_1 + 2\kappa_0\kappa_2)A_n \cos(n\pi z)e^{ik_n x} \tag{21a}$$

$$\Psi_2'(0) = -\frac{1}{2} \left(p_2^2(b_{21} + b_{22}) - p_3^2(b_{31} + b_{32}) \right) + \frac{i}{2} \frac{C_{66}}{C_{44}} k_s ((k_n + k_s)(b_{21} + b_{22}) + (k_n - k_s)(b_{31} + b_{32})) \tag{21b}$$

$$\Psi_2'(1)e^{ik_n x} = -\frac{\delta}{2} \left(p_2^2(b_{21}e^{ip_2} + b_{22}e^{-ip_2})e^{-i\theta} - p_3^2(b_{31}e^{ip_3} + b_{32}e^{-ip_3})e^{i\theta} \right) + \frac{i\delta}{2} \frac{C_{66}}{C_{44}} k_s \left((k_n + k_s)(b_{21}e^{ip_2} + b_{22}e^{-ip_2})e^{-i\theta} + (k_n - k_s)(b_{31}e^{ip_3} + b_{32}e^{-ip_3})e^{i\theta} \right) \tag{21c}$$

If the governing equation (21a) is multiplied by $\cos(n\pi z)$ and integrated by parts from $z = 0$ to $z = 1$, and then the boundary conditions (21b, 21c) are invoked. One obtains the second-order correction for the wavenumber as $\kappa_2 = [\Psi_2'(0) - \Psi_2'(1) \cos(n\pi)]/2\kappa_0$. Thus, the asymptotically approximate value of the wavenumber of the SH wave in the corrugated plate is

$$\kappa \approx \sqrt{(n\pi)^2 + Rk_n^2} + \varepsilon^2 \left[\frac{\Psi_2'(0) - \Psi_2'(1) \cos(n\pi)}{2\kappa_0} \right] \tag{22}$$

Having obtained the nondimensional shear wavenumber in the weakly corrugated plate, one can estimate the phase velocity of the ultrasonic shear wave from the following relationship:

$$c = \omega / Re(\kappa/\hat{h}) \tag{23}$$

3 Discussion and Illustrations

The periodically corrugated plates considered for numerical illustrations are all made of an elastic material with a density of $\rho = 4.4 \text{ g/cm}^3$ and elastic shear moduli of $C_{44} = 60 \text{ GPa}$ and $C_{66} = 40 \text{ GPa}$. The periodic surfaces have nondimensional wavenumbers (k_s) between 1 and 10. During calculation, stopband frequency domains, centered at $k_s = \kappa/2$, are avoided so that transmission within passbands is considered. Two ratios of the amplitude of surface corrugation to the average thickness of the plates (ε) are taken to be 0.005 or 0.01. It is the aim of this research to investigate the influence of the combined effects of surface corrugations and initial stress; the illustrations are presented in three scenarios. 1) Plates having the same periodic surface wavenumber, same corrugation amplitude, and different initial stresses. 2) Plates having the same periodic surface wavenumber, different corrugation amplitudes, and positive or negative initial stresses. 3) Plates having various periodic surface wavenumbers, same corrugation amplitude, and positive or negative initial stresses.

Figure 2 shows the fundamental SH mode of a shear wave propagating along an axis of material symmetry in a plate with smooth surfaces to be nondispersive. The plate is, however, dispersive when its surfaces are uneven, as shown for the fundamental SH modes of periodic plates with (ε) equals to 0.005 or 0.01. In fact, the higher-amplitude surface-corrugated plate is the stronger dispersion the plate has. This dispersive nature of the fundamental SH mode is predicted by Eq. (22), which provides an asymptotic estimation of the wavenumber. Therefore, estimation of the behavior of SH waves propagating in plates with surface corrugation must be

obtained by considering the second-order perturbation solution.

Next, let us consider the influence of plate surface corrugation wavenumber on the fundamental SH mode phase speed in an initial stress-free periodic plate. At 1 kHz, as a representative case shown in Fig. 3, the shear wave travels slower in the corrugated plate having high periodic corrugation wavenumber (corresponding to a small surface wavelength, which resembles the case of a plate with periodic surface roughness) than it does in the corrugated plate having low periodic corrugation wavenumber (corresponding to large surface wavelength, which resembles the case of a plate surface with weak waviness).

The effect of initial stress on the dispersive behavior of periodically corrugated plates is investigated. Calculations are done for three corrugated plates with a surface nondimensional wavenumber of ten. One of the plates is laid under initial compression of 1 GPa, one of them is placed under initial tension of 1 GPa, and one plate does not have any initial stress. Figure 4 indicates the fact that the ultrasonic SH0 mode travels slightly slower in the initially compressed periodically corrugated plate than it does in the stress-free periodic plate. In addition, the SH0 mode travels slightly faster in the periodically corrugated plate subjected to initial tensile stress than it does in the stress-free periodic plate. It is also worth reporting that the more initial compressive stress the periodic plate has, the lower the phase velocity the shear wave travels in it, and the stronger initial tensile stress the periodic plate has, the higher the phase velocity the wave travels in it. A point one can note is that dispersion curves of the periodically corrugated plates are all asymptotically approaching the bulk shear phase speed of the plate material,

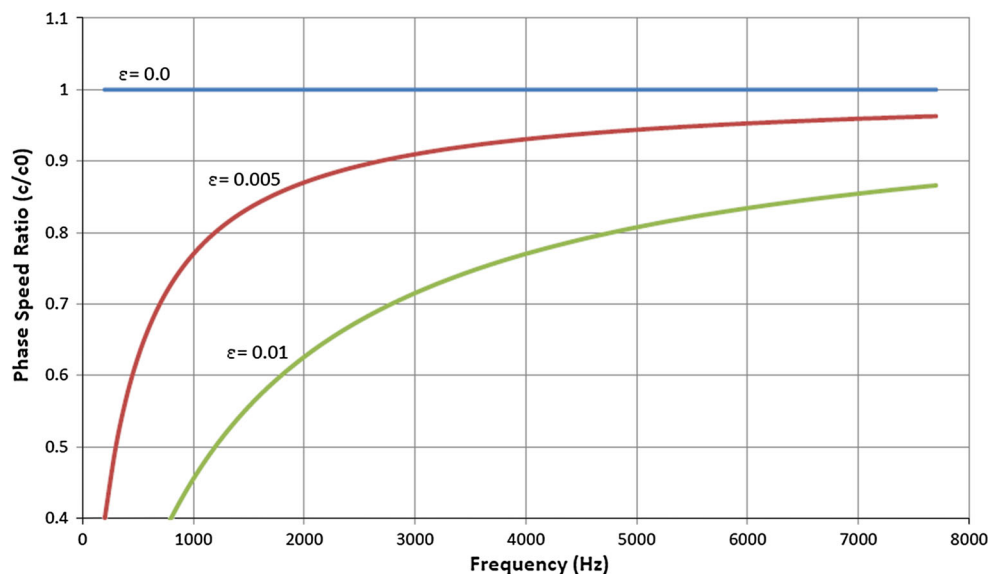


Fig. 2 Phase velocities of an ultrasonic fundamental SH mode propagating in plates with no initial stress and different periodic surface corrugation amplitude levels. $h = 1 \text{ mm}$, $k_s = 5.0$, $\theta = 90^\circ$, and $\delta = 1$

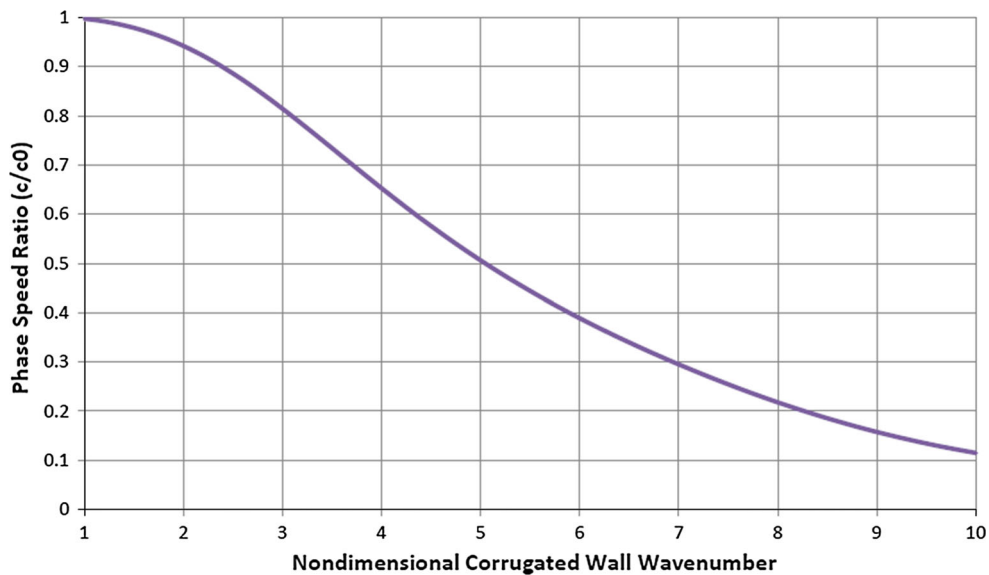


Fig. 3 Phase velocities of an ultrasonic fundamental SH mode at 1 kHz propagating in plates with different periodically corrugated surface wavenumbers and carrying no initial stress. $h = 1 \text{ mm}, \varepsilon = 0.01, \theta = 90^\circ$, and $\delta = 1$

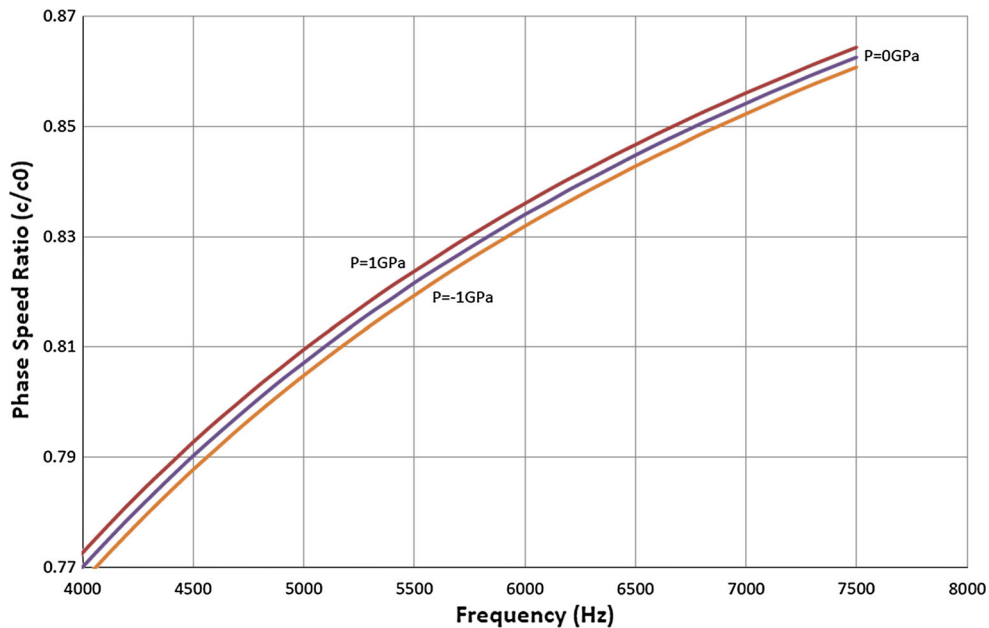


Fig. 4 Phase velocities of an ultrasonic fundamental SH mode propagating in corrugated plates under indicated tensile/compressive initial stresses. $h = 1 \text{ mm}, k_s = 10.0, \theta = 90^\circ$, and $\delta = 1$

$c_0 = \sqrt{C_{44}/\rho}$, that is equal to 3692 m/s at a high frequency. A physical interpretation of material behavior can be made in light of the fact that tensile stresses pull material particles apart from each other, forming in a way a less dense continuum. Waves travel faster in media with low density. Compressive stresses, on the other hand, cause an opposite effect.

The magnitude of initial stress in the giga Pascal range is somehow exaggerated compared to realistic ultimate shear strengths in the mega Pascal range. The choice of 1GPa as

an initial stress value is based on the fact that lower levels of initial stresses unnoticeably alter the dispersion curve of the stress-free periodic plate. The observations made in Fig. 4 go along with the findings of previous studies by Zhuk [2], who studies SH waves in an elastic layer with smooth surfaces under initial extension across its thickness. Results are also in agreement with Son and Kang [23] who considered SH waves in a composite plate with smooth surfaces under initial stresses of more than $|10^8| \text{ Pa}$ along the plate, in the wave propagation direction.

Fig. 5 Difference (at various frequencies) between phase velocities of an ultrasonic fundamental SH mode propagating in corrugated plates under indicated tensile/compressive initial stresses. $h = 1$ mm, $k_s = 10.0$, $\theta = 90^\circ$, and $\delta = 1$

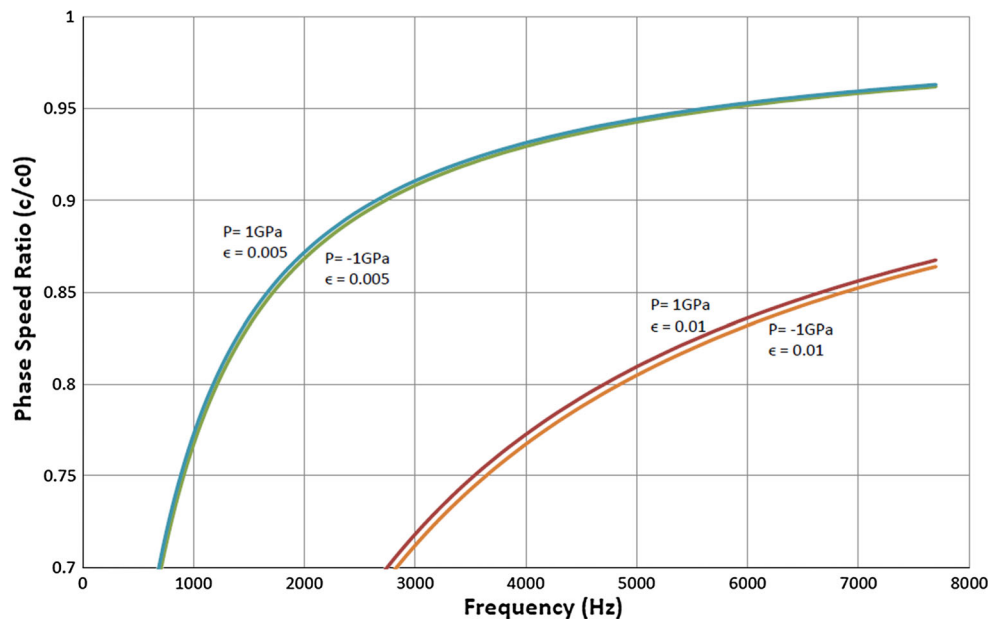
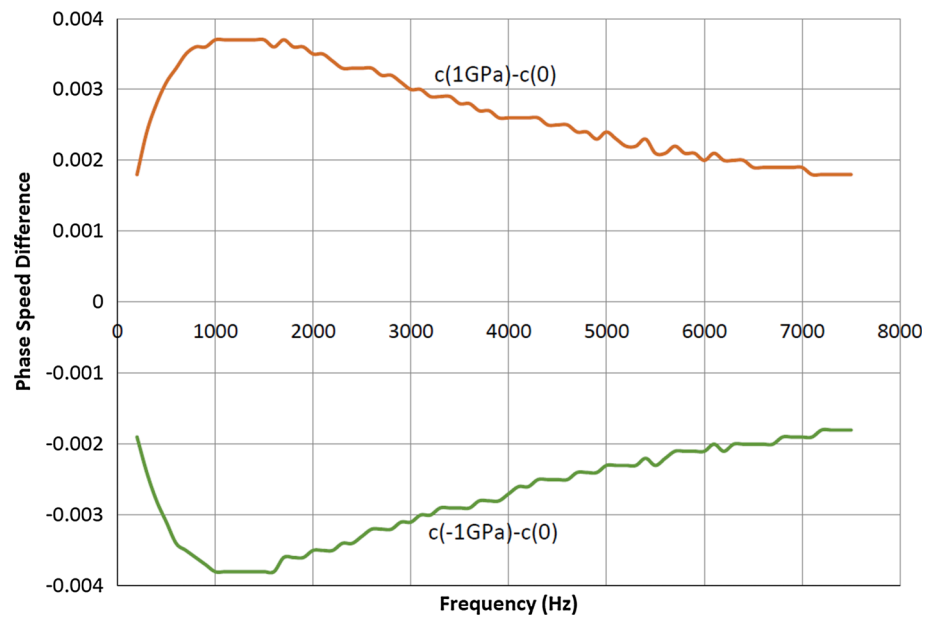


Fig. 6 Phase velocities of an ultrasonic fundamental SH mode propagating in corrugated plates under indicated tensile/compressive initial stresses and indicated corrugation amplitudes. $h = 1$ mm, $k_s = 10.0$, $\theta = 90^\circ$, and $\delta = 1$

The difference between fundamental SH phase speed in a periodically corrugated plate under initial tensile (compressive) stress of 1GPa (-1GPa) and that in a stress-free periodically corrugated plate is shown in Fig. 5. One can conclude that the effect of initial stresses on the SH0 phase speed gets weaker at higher frequencies.

In order to measure the combined effect of periodic corrugation strength and the initial tension/compression stress of ∓ 1 GPa, let us consider two periodically corrugated plates with amplitude ratios (ϵ) of 0.005 and 0.01, and let each of

these plates be under initial compressive stress in one situation and under initial tensile stress in the other. Figure 6 shows that the SH0 phase velocities in the plate with higher corrugation amplitude are lower than the phase velocities in the plate with lower corrugation amplitude. Hence, conclusions derived from Fig. 2 are applicable for the cases of periodically corrugated plates under initial stresses. Therefore, stronger corrugations lead to higher levels of interaction between propagating shear waves and the initially stressed plate geometric inhomogeneity. In addition, similar obser-

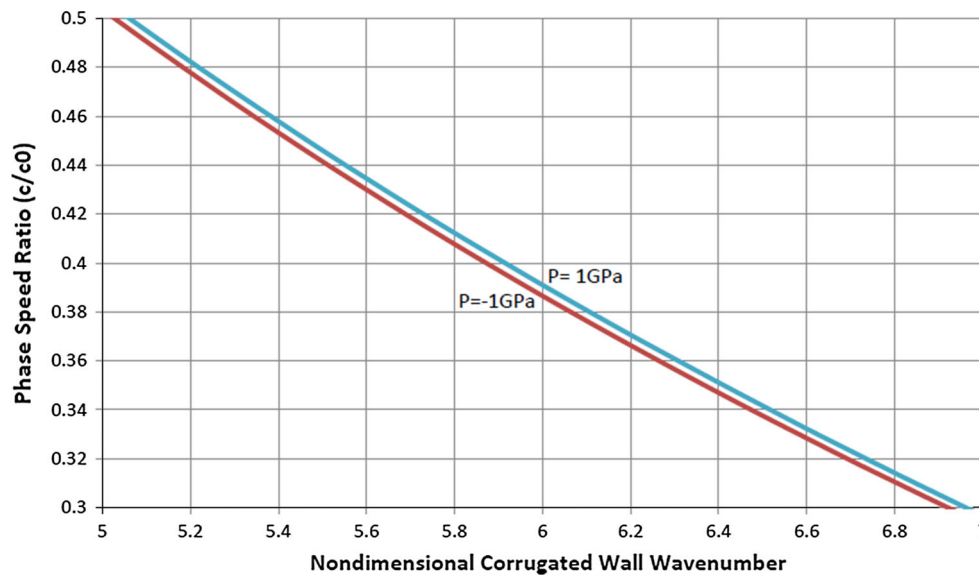


Fig. 7 Phase velocities of an ultrasonic fundamental SH mode propagating in initially stressed plates with different periodically corrugated surface wavenumbers. $h = 1$ mm, $\varepsilon = 0.01$, $\theta = 90^\circ$, and $\delta = 1$

vation to that made in Fig. 4 is noted here; ultrasonic shear signals travel slightly faster in the periodic plate when subjected to initial tensile stress than they do in the periodic plate that is put under initial compression.

Figure 7 shows the relationship between the fundamental SH mode phase speed and the periodic surface corrugation wavenumber in two periodically corrugated plates; one of them is under initial compression, and the second plate is under initial tension. At all frequencies, shear signals in the plate under initial tension propagate at higher velocities than that in these propagating in the plate under initial compression. From Figs. 6 and 7, one can construe that periodic surface roughness has a stronger effect on reducing SH0 phase speeds than a weak surface waviness does.

4 Conclusion

In this paper, an asymptotic analysis up to the second order was presented for studying the influence of initial stress on shear wave propagation in elastic plates with periodically corrugated free surfaces. The derived asymptotic expressions were graphically presented to study the combined influence of the geometric inhomogeneity and initial compressive or tensile stresses. Initial stress effect on phase speeds of the shear wave was very small. The density of periodic surface corrugation was found to have an effect on the phase velocity of propagating shear waves. It was shown that surface corrugations having small wavelengths had a stronger effect on reducing wave phase speeds than surface corrugations having large wavelengths. The effect of tensile and compressive initial stresses on shear phase speeds decreases

at higher frequencies. The study quantified the influence of large corrugation amplitude in comparison with small corrugation amplitudes. The study showed that ultrasonic shear signals travelled faster in plates under initial tension than they did in initially compressed plates.

Acknowledgements Research support offered by King Fahd University of Petroleum and Minerals (KFUPM) is acknowledged.

References

1. Wagh, D.K.: Propagation of SH waves in an infinite elastic plate with Cauchy's initial transverse stress. *Pure Appl. Geophys.* **99**, 49–54 (1972)
2. Zhuk, A.P.: Propagation of SH waves and torsional waves in an infinite elastic layer with initial stresses. *Prikl. Mekhanika* **11**, 17–21 (1975)
3. Wilson, A.J.: Wave propagation in thin pre-stressed elastic plates. *Int. J. Eng. Sci.* **15**, 245–251 (1977)
4. Ogden, R.W.; Roxburgh, D.G.: The effect of pre-stress on the vibration and stability of elastic plates. *Int. J. Eng. Sci.* **30**, 1611–1639 (1993)
5. Roxburgh, D.G.; Ogden, R.W.: Stability and vibration of pre-stressed compressible elastic plates. *Int. J. Eng. Sci.* **32**, 427–454 (1994)
6. Rogerson, G.A.; Fu, Y.B.: An asymptotic analysis of the dispersion relation for a pre-stressed incompressible elastic plate. *Acta Mech.* **111**, 59–74 (1995)
7. Sandiford, K.J.; Rogerson, G.A.: Some dynamic properties of a pre-stressed, nearly incompressible (rubber-like) elastic layer. *Int. J. Non Linear Mech.* **35**, 849–868 (2000)
8. Pichugin, A.V.: Asymptotic Models for Long Wave Motion in a Pre-stressed Incompressible Elastic Plate. Ph.D. Dissertation, Salford University, UK (2001).
9. Kaplunov, Y.D.; Nolden, Y.V.: Long-wave vibrations of a nearly incompressible isotropic plate with fixed faces. *Q. J. Mech. Appl. Math.* **55**, 345–356 (2001)

10. Kaplunov, J.D.; Nolde, E.V.; Rogerson, G.A.: An asymptotically consistent model for long wave high frequency motion in a pre-stressed elastic plate. *Math. Mech. Solids* **7**, 581–606 (2002a)
11. Kaplunov, J.D.; Nolde, E.V.; Rogerson, G.A.: Short wave motion in a pre-stressed elastic plate. *IMA J. Appl. Math.* **67**, 383–399 (2002b)
12. Nolde, E.V.; Prikazchikova, L.A.; Rogerson, G.A.: Dispersion of small amplitude waves in a pre-stressed, compressible elastic plate. *J. Elast.* **75**, 1–29 (2004)
13. Wijeyewickrema, A.C.; Ushida, Y.; Kayestham, P.: Wave propagation in a pre-stressed compressible elastic layer with constrained boundaries. *J. Mech. Mater. Struct.* **3**, 1963–1976 (2008)
14. Zhang, X.M.; Yu, J.G.: Effects of initial stresses on guided waves in unidirectional plates. *Arch. Mech.* **65**, 3–26 (2013)
15. Pau, A.; di Scalea, F.L.: Nonlinear guided wave propagation in prestressed plates, top of form bottom of form. *J. Acoust. Soc. Am.* **137**, 1529–1540 (2015)
16. Rogerson, G.A.; Sandiford, K.J.: On small amplitude vibrations of pre-stressed laminates. *Int. J. Eng. Sci.* **34**, 853–872 (1996)
17. Akbarov, S.D.; Zamanov, A.D.; Agasiyev, E.R.: On the propagation of Lamb waves in a sandwich plate made of compressible materials with finite initial strains. *Mech. Compos. Mater.* **44**, 155–164 (2008)
18. Wijeyewickrema, A.C.; Leungvichcharoen, S.: Wave propagation in pre-stressed imperfectly bonded compressible elastic layered composites. *Mech. Mater.* **41**, 1192–1203 (2009)
19. Kayestha, P.; Wijeyewickrema, A.C.: Time-harmonic wave propagation in a prestressed compressible elastic bi-material laminate. *Eur. J. Mech. A/Solids* **29**, 143–151 (2010)
20. Kayestha, P.; Wijeyewickrema, A.C.; Kishimoto, K.: Wave propagation along a non-principal direction in a compressible pre-stressed elastic layer. *Int. J. Solids Struct.* **48**, 2141–2153 (2011)
21. Zamanov, A.D.; Agasiyev, E.R.: Dispersion of lamb waves in a three-layer plate made from compressible materials with finite initial deformations. *Mech. Compos. Mater.* **46**, 583–592 (2011)
22. Akbarov, S.D.; Agasiyev, E.R.; Zamanov, A.D.: Wave propagation in a pre-strained compressible elastic sandwich plate. *Eur. J. Mech. A/Solids* **30**, 409–422 (2011)
23. Son, M.S.; Kang, Y.J.: The effect of initial stress on the propagation behavior of SH waves in piezoelectric coupled plates. *Ultrasonics* **51**, 489–495 (2011)
24. Yu, J.; Li, S.: Dispersion of guided waves in initially stressed layered plates. *J. Mech. Mater. Struct.* **8**, 185–198 (2013)
25. Biot, A.M.: *Mechanics of Incremental Deformations*. Wiley, New York (1965)
26. Nayfeh, A.H.: *Introduction to Perturbation Techniques*. Wiley-Interscience, New York (1981)
27. Elachi, C.: Waves in active and passive periodic structures: a review. *Proc. IEEE* **64**, 1666–1698 (1976)
28. Hawwa, M.A.; Asfar, O.R.: Mechanical-wave filtering in a periodically corrugated elastic plate. *ASME J. Vib. Acoust.* **18**, 16–20 (1996)
29. Hawwa, M.A.: Acoustic/ultrasonic mode coupling in waveguides involving two periodicities. *J. Acoust. Soc. Am.* **102**, 137–142 (1997)

